

Quantum logic operations and creation of entanglement in a scalable superconducting quantum computer with long-range constant interaction between qubits

G. P. Berman¹, A. R. Bishop¹, D. I. Kamenev¹, and A. Trombettoni^{1,2}

¹*Theoretical Division, Los Alamos National Laboratory, Los Alamos, New Mexico 87545 and*

²*I.N.F.M. and Dipartimento di Fisica, Università di Parma,*

parco Area delle Scienze 7A Parma, I-43100, Italy

We consider a one-dimensional chain of many superconducting quantum interference devices (SQUIDs), serving as charge qubits. Each SQUID is coupled to its nearest neighbors through constant capacitances. We study the quantum logic operations and implementation of entanglement in this system. Arrays with two and three qubits are considered in detail. We show that the creation of entanglement with an arbitrary number of qubits can be implemented, without systematic errors, even when the coupling between qubits is not small. A relatively large coupling constant allows one to increase the clock speed of the quantum computer. We analytically and numerically demonstrate the creation of the entanglement for this case, which can be a good test for the experimental implementation of a relatively simple quantum protocol with many qubits. We discuss a possible application of our approach for implementing universal quantum logic for more complex algorithms by decreasing the coupling constant and, correspondingly, decreasing the clock speed. The errors introduced by the long-range interaction for the universal logic gates are estimated analytically and calculated numerically. Our results can be useful for experimental implementation of quantum algorithms using controlled magnetic fluxes and gate voltages applied to the SQUIDs. The algorithms discussed in this paper can be implemented using already existing technologies in superconducting systems with constant inter-qubit coupling.

PACS numbers: 03.67.Lx, 75.10.Jm, 85.25.Dq

I. INTRODUCTION

In the last few years, a large number of studies has been devoted to the realization of qubits using Josephson devices [1]. A single superconducting qubit can be realized using either charge or flux degrees of freedom. The flux Josephson two-state system is based on two quantum states carrying opposite persistent currents. Coherent time evolution between these states has been recently observed [2]. At present, however, no quantum oscillations between two coupled flux qubits has been reported. In charge Josephson qubits the relevant degree of freedom is the charge on superconducting grains. The coherent control of macroscopic quantum states in a single Cooper-pair box has been demonstrated [3], while the first observation of coherent quantum oscillations in two coupled charge qubits has been reported [4]. Moreover, coherent oscillations have been observed in other superconducting devices [5, 6, 7]. While longer coherence times are desirable, these experiments show that the superconducting circuits are strong candidates for solid-state qubits. The next major step toward building a Josephson-junction based quantum computer is to experimentally realize simple quantum algorithms, such as the creation of an entangled state involving more than two coupled qubits.

A typical design of a Cooper pair box consists of a small superconducting island with n Cooper pair charges connected by a tunnel junction with a Josephson coupling energy E_J and the capacitance C_J to a superconducting electrode [1]. A control gate voltage V is coupled to the system via a gate capacitor C_g .

The energy of the n Cooper pairs in the box is $E = 4E_C n^2 - 2enV$, where $E_C = e^2/2(C_g + C_J)$, and e is the electron charge. Considering later n as one of the canonical variables, and neglecting the constant term, we can represent E in the form $E = 4E_C(n - n_g)^2$, where $n_g = C_g V/2e$ is the gate charge (in units of $2e$). When $E_C \gg E_J$, by choosing n_g close to the degeneracy point, $n_g = (2n + 1)/2$, only the states with n and $n + 1$ Cooper pairs play a role. In this case, the effective Hamiltonian of the two-state system can be written in the spin- $\frac{1}{2}$ notation as

$$\bar{\mathbf{H}}_1 = -\bar{B}^z \mathbf{S}^z - B^x \mathbf{S}^x, \quad (1)$$

where the state with n Cooper pairs corresponds to the spin state $\begin{pmatrix} 1 \\ 0 \end{pmatrix}$ and the state with $n + 1$ Cooper pairs corresponds to the spin state $\begin{pmatrix} 0 \\ 1 \end{pmatrix}$ (see, for example, [1]); \mathbf{S}^z and \mathbf{S}^x are,

respectively, the z and x - components of spin- $\frac{1}{2}$ operator; $\bar{B}_z \sim 4E_c(1 - 2n_g)$ and $B_x \sim E_J$ are the effective magnetic fields which are controlled by the applied gate voltage and the magnetic flux. [See Eqs. (8) below.]

The Hamiltonian of an array of coupled superconducting qubits can be written in the general form

$$\bar{\mathbf{H}} = - \sum_{i=0}^{N-1} \bar{B}_i^z \mathbf{S}_i^z - \sum_{i=0}^{N-1} B_i^x \mathbf{S}_i^x + \sum_{\substack{i,j=0 \\ i \neq j}}^{N-1} U_{ij}^a \mathbf{S}_i^a \mathbf{S}_j^b, \quad (2)$$

where $a = x, y, z$ and N is the number of qubits in the circuit. The explicit form of the coefficients U_{ij}^a in (2) depends on the particular way in which the inter-qubit coupling is implemented. A variety of possible architectures to couple charge Josephson qubits has been proposed [8, 9, 10, 11, 12, 13, 14]. It has been suggested [8] to realize a coupling of the type $\propto \mathbf{S}_i^y \mathbf{S}_j^y$ using an inductor: all qubits were connected in parallel to an LC-oscillator which provided the two-qubit interaction. A possible limitation of this architecture is that the inter-qubit coupling term is valid only under the conditions that the phase conjugate to the total charge on the qubit capacitors fluctuates weakly, and that the eigenfrequency ω_0 of the LC circuit is much larger than the typical frequencies of the qubit dynamics. Since ω_0 scales with the number N of qubits as $1/\sqrt{N}$, this limits the maximum number of qubits in the quantum register. A different proposed type of the inter-qubit coupling uses the Coulomb interaction between charges on the islands of the charge qubits [9]: this gives a coupling $\propto \mathbf{S}_i^z \mathbf{S}_j^z$. A drawback of this approach is that one cannot switch the inter-qubit coupling in this scheme without introducing unwanted dephasing effects. Another proposed architecture employs two additional SQUIDs to connect each qubit: all Josephson charge qubits are coupled through a common superconducting inductance, and the resulting coupling is $\propto \mathbf{S}_i^x \mathbf{S}_j^x$ [11]. The same coupling of charge qubits can also be realized using mutual inductance [10]. Finally, we mention that another experimental realization of a single superconducting charge qubit has been obtained using the current-biased Josephson junctions [6, 7]. A quantum computer architecture based on two capacitively coupled current-biased Josephson junctions was discussed before [12, 13, 14].

In this paper, we consider capacitively coupled SQUIDs, which currently are the only experimental setup that has provided an experimental detection of quantum oscillations in two coupled charge qubits [4]. In this architecture, the SQUIDs are connected via a constant capacitor, and the coupling is of the form $\propto \mathbf{S}_i^z \mathbf{S}_j^z$. Varying the magnetic flux Φ through the

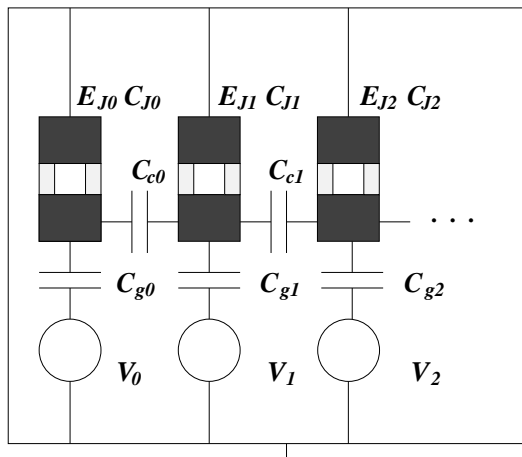


FIG. 1: A schematic illustration of array of capacitively coupled SQUIDs.

SQUIDs allows one to control the Josephson energy E_J , which is equivalent to controlling the effective magnetic field B^x [1]. Therefore, we will assume that it is possible to have the Josephson energies [*i.e.*, B_i^x coefficients in Eq.(2)] independently and locally variable in time.

We note that experimentally the fast independent manipulation of gate voltages is possible [15, 16]. At the same time, the fast independent control of magnetic fluxes through the different SQUIDs with the distance $\sim 1 \mu\text{m}$ between them and the switching time $\sim 1 \text{ ns}$ represents a challenge to the present-day technology. As an alternative, the B^x field can be manipulated by using recently proposed [17] Nb/ AlO_x Nb-Al/ AlO_x /Nb stacked Josephson junctions instead of SQUIDs. In the double Josephson junction device, injection current I_{inj} (of the order of several mA) in the control junction induces variation of the Josephson critical current I_c (of the order of several μA). As for a single Josephson junction $B_x \sim E_J = I_c \Phi^0 / (2\pi c)$ ($\Phi^0 = hc/2e$ is the flux quantum, h is the Planck's constant, and c is the light velocity) manipulation of I_c allows one to control the B^x field. In the experiment [17] $I_c = 0$ (and $B^x = 0$) for $I_{inj} \approx 2.5 \text{ mA}$. Using the electrical signals instead of the localized magnetic fluxes for controlling the B^x field would allow one to speed up the quantum computer operations and to simplify the design. The results presented in this paper are applicable also to the quantum computer based on the stacked Josephson junctions (instead of SQUIDs) serving as qubits.

II. ARRAY OF CAPACITIVELY COUPLED SQUIDS AS A QUANTUM REGISTER

A schematic plot of an array of N capacitively coupled SQUIDS is shown in Fig. 1. The i th SQUID with $i = 0, \dots, N-1$ corresponds to the i th qubit. The SQUIDS have Josephson energies E_{J_i} and capacitances C_{J_i} . Each SQUID is connected to the control gate voltages V_i via a gate capacitor C_{g_i} . The i th intermediate qubit is connected to its two neighboring ($i \pm 1$)th qubits via the capacitors $C_{i,i\pm 1}$, where $C_{i,i+1}$ are the off-diagonal elements of the capacitance matrix. In Fig. 1 we use the notation $C_{ci} = C_{i,i+1}$. The end 0th and $(N-1)$ th SQUIDS are connected to one, respectively, the 1st and $(N-2)$ th SQUIDS. The Hamiltonian corresponding to the charging energy of this system can be written as

$$\mathbf{H}_C(t) = 4 \sum_{i,j=0}^{N-1} [\mathbf{n}_i - n_{g_i}(t)] \Gamma_{ij} [\mathbf{n}_j - n_{g_j}(t)], \quad (3)$$

where \mathbf{n}_i is the operator for the total number of Cooper pairs in the i th SQUID, and $n_{g_i}(t) = C_{g_i} V_i(t)/2e$ is the charge (in units of $2e$) induced on the i -th qubit by the corresponding dc electrode; Γ_{ij} is related to the inverse of the capacitance matrix C_{ij} of the system by

$$\Gamma_{ij} = \frac{e^2}{2} C_{ij}^{-1}. \quad (4)$$

To illustrate the structure of the capacitance matrix we assume that all SQUIDS are identical with the same capacitances $C_{g_i} = C_g$, $C_{J_i} = C_J$, and $C_{ci} = C_c$. (This assumption is made for this example only.) Then, the capacitance matrix is

$$C_{ij} = C_0 \left[\delta_{ij} (1 + g\eta) - \eta \sum_d \delta_{i,i+d} \right], \quad (5)$$

where $C_0 = C_g + C_J$, $\eta = C_c/C_0$; δ_{ij} is the Kronecker delta-symbol; $d = \pm 1$ and $g = 2$ for the intermediate qubits; $d = 1$ and $g = 1$ for the 0th qubit; $d = -1$ and $g = 1$ for the last $(N-1)$ th qubit. If other devices (for measurement) are attached to the SQUIDS, their capacitances must be added to C_0 .

Since the matrix Γ_{ij} is the inverse of a tridiagonal matrix, it has nonzero matrix elements on the second, third and other diagonals which characterize the long-range interaction between the qubits. However, for $\eta \ll 1$ the off-diagonal elements of Γ_{ij} decay exponentially as $\eta^{|i-j|}$, so that the influence of the long-range interaction can be reduced by taking the coupling capacitances C_c to be much smaller than the on-site capacitances C_0 . (In the experiment [4] the value of η was chosen to be $\eta \sim 0.05$.)

Usually, long-range interaction between qubits is difficult to control, and this interaction represent a problem for quantum computation. However, in the case when there are only two states in the quantum register, we will show that the destructive effect of the long-range interaction can be completely suppressed by the proper choice of protocol parameters, so that the condition $\eta \ll 1$ is not required in this case. Since the clock speed of the quantum computer is proportional to η , increasing the value of η would allow one to increase the speed of implementation of a quantum algorithm. This particular example with two states can be important for benchmarking a scalable superconducting quantum computer device.

In order to obtain the effective Hamiltonian in spin- $\frac{1}{2}$ notation (see, for example, [18, 19]), we make the substitution $n_{gi} = n_i^0 + m_{gi}$ and $\mathbf{n}_i = n_i^0 + \mathbf{m}_i$, where \mathbf{m}_i is the operator of excess number of Cooper pairs on i th SQUID. The dimensionless charging Hamiltonian (3) becomes

$$\mathbf{H}'_C(t) = \frac{C_0}{2e^2} \mathbf{H}_C(t) = \sum_{i,j=0}^{N-1} [\mathbf{m}_i - m_{gi}(t)] U_{ij} [\mathbf{m}_j - m_{gj}(t)], \quad (6)$$

where $U_{ij} = \Gamma_{ij} C_0 / (2e^2)$ and C_0 is the on-site capacitance for the 0th qubit. It is convenient to introduce the spin operator $\mathbf{S}_i^z = 1/2 - \mathbf{m}_i$ with projections $s_i^z = \pm 1/2$ on the z -axis. We treat \mathbf{m}_i as an operator with eigenvalues 0 and 1. Then, the state with the eigenvalue $m_i = 0$ corresponds to the spin state $\begin{pmatrix} 1 \\ 0 \end{pmatrix}$, and the state with the eigenvalue $m_i = 1$ corresponds to the spin state $\begin{pmatrix} 0 \\ 1 \end{pmatrix}$ [1]. Using the relation between \mathbf{m}_i (\mathbf{m}_j) and \mathbf{S}_i^z (\mathbf{S}_j^z), the symmetry property $U_{ij} = U_{ji}$, and the fact that $(\mathbf{S}_i^z)^2 = \frac{1}{4} \begin{pmatrix} 1 & 0 \\ 0 & 1 \end{pmatrix}$, the Hamiltonian of the whole system can be written in the form

$$\mathbf{H}(t) = - \sum_{i=0}^{N-1} \bar{B}_i^z(t) \mathbf{S}_i^z - \sum_{i=0}^{N-1} B_i^x(t) \mathbf{S}_i^x + \sum_{\substack{i,j=0 \\ i \neq j}}^{N-1} U_{ij} \mathbf{S}_i^z \mathbf{S}_j^z. \quad (7)$$

Here we omitted the term $\sum_{i,j=0}^{N-1} U_{ij} [m_{gi}(t) - 1/2][m_{gj}(t) - 1/2] + (1/4) \sum_{i=0}^{N-1} U_{ii}$, which does not contain the spin operators and does not influence the quantum equations of motion.

The controllable \bar{B}^z and B^x fields are expressed through the parameters of the model:

$$\bar{B}_i^z(t) = \sum_{j=0}^{N-1} U_{ij} [1 - 2m_{gj}(t)], \quad B_i^x(t) = \frac{C_0}{2e^2} E_{Ji} [\Phi_i(t)] = \frac{C_0}{e^2} E_{Ji}^0 \cos[\pi \Phi_i(t) / \Phi^0], \quad (8)$$

where E_{Ji}^0 is the Josephson energy of each of the two Josephson junctions of the i -th SQUID, $\Phi_i(t)$ is the magnetic flux through the i -th SQUID. From the second expression in Eq. (8) it follows that $B_i^x = 0$ for non-zero flux $\Phi_i = (2k - 1)\Phi^0/2$, where $k = 1, 2, \dots$

A. Two qubits

Some basic properties of the system can be understood from an exact analysis of the SQUID chains containing two or three qubits. For the system of two capacitively coupled qubits, the capacitance matrix is

$$C_{ij} = \begin{pmatrix} C_0 + C_c & -C_c \\ -C_c & C_1 + C_c \end{pmatrix} = C_0 \begin{pmatrix} 1 + \eta & -\eta \\ -\eta & a + \eta \end{pmatrix}, \quad (9)$$

where $a = C_1/C_0$; $C_0 = C_{g0} + C_{J0}$ is the on-site capacitance for the 0th qubit; and $C_1 = C_{g1} + C_{J1}$ is the on-site capacitance for the 1st qubit. The matrix U_{ij} has the form

$$U_{ij} = \frac{1}{a + (1 + a)\eta} \begin{pmatrix} a + \eta & \eta \\ \eta & 1 + \eta \end{pmatrix}. \quad (10)$$

Since the coupling constant $U_{01} = \eta/[a + (1 + a)\eta]$ is positive, the coupling in the system is antiferromagnetic. This is also true for larger qubit arrays.

B. Three qubits

Assuming that all on-site capacitances and coupling capacitances are the same for all SQUIDs (we make this assumption only for this particular example), the capacitance matrix for the system of three qubits is

$$C_{ij} = \begin{pmatrix} C_0 + C_c & -C_c & 0 \\ -C_c & C_0 + 2C_c & -C_c \\ 0 & -C_c & C_0 + C_c \end{pmatrix} = C_0 \begin{pmatrix} 1 + \eta & -\eta & 0 \\ -\eta & 1 + 2\eta & -\eta \\ 0 & -\eta & 1 + \eta \end{pmatrix}. \quad (11)$$

The matrix U_{ij} has the form

$$U_{ij} = \frac{1}{1 + 4\eta + 3\eta^2} \begin{pmatrix} 1 + 3\eta + \eta^2 & \eta + \eta^2 & \eta^2 \\ \eta + \eta^2 & 1 + 2\eta + \eta^2 & \eta + \eta^2 \\ \eta^2 & \eta + \eta^2 & 1 + 3\eta + \eta^2 \end{pmatrix}. \quad (12)$$

For the system of three qubits the coupling constants are

$$U_{01} = U_{12} = \frac{\eta + \eta^2}{1 + 4\eta + 3\eta^2}, \quad U_{02} = \frac{\eta^2}{1 + 4\eta + 3\eta^2}. \quad (13)$$

As mentioned above, the off-diagonal matrix elements $U_{i,j}$ decrease approximately as $\eta^{|i-j|}$, where $\eta \ll 1$. The diagonal components $U_{i,i}$, which affect the field field \bar{B}_i^z in the first expression in Eq. (8), depend on the position of the qubit in the chain, i . For a system consisting of larger number of qubits, the off-diagonal components also depend on i .

III. THE \mathbf{B}_i^z OPERATOR FIELD

It is convenient to express the Hamiltonian (7) in terms of the operator field $\mathbf{B}_i^z(t)$,

$$\mathbf{H}(t) = - \sum_{i=0}^{N-1} \mathbf{B}_i^z(t) \mathbf{S}_i^z - \sum_{i=0}^{N-1} B_i^x(t) \mathbf{S}_i^x, \quad (14)$$

$$\mathbf{B}_i^z(t) = \sum_{\substack{j=0 \\ j \neq i}}^{N-1} \left\{ U_{ij} \left[1 - 2m_{gj}(t) - \mathbf{S}_j^z \right] \right\} + U_{ii} [1 - 2m_{gi}(t)]. \quad (15)$$

Here different terms correspond to different sources of the $\mathbf{B}_i^z(t)$ field in the location of i th qubit. The term $U_{ij}[1 - 2m_{gj}(t)]$ is the field produced by the application of the voltage to the j th qubit, $j \neq i$; the term $U_{ii}[1 - 2m_{gi}(t)]$ is the field created by applying the voltage directly to the i th qubit; and the term $-U_{ij}\mathbf{S}_j^z$, $j \neq i$, is the field produced by the j th qubit in the location of the i th qubit due to the constant interaction between them.

Since the $\mathbf{B}_i^z(t)$ field is an operator, it generates different actual B_i^z fields for different states. The B_i^z field $B_i^z(p, t)$ in the location of the i th qubit for the state $|p\rangle$ is defined as

$$B_i^z(p, t) = \langle p | \mathbf{B}_i^z | p \rangle = \sum_{\substack{j=0 \\ j \neq i}}^{N-1} \left\{ U_{ij} \left[1 - 2m_{gj}(t) - s_j^z(p) \right] \right\} + U_{ii} [1 - 2m_{gi}(t)], \quad (16)$$

where $s_j^z(p)$ is the eigenvalue of \mathbf{S}_j^z for the state $|p\rangle$. For example, for the state $|0\rangle = |00 \dots 00\rangle$ one has $s_j^z(0) = 1/2$ for all j 's and

$$B_i^z(0, t) = \langle 0 | \mathbf{B}_i^z | 0 \rangle = \sum_{\substack{j=0 \\ j \neq i}}^{N-1} \left\{ U_{ij} \left[\frac{1}{2} - 2m_{gj}(t) \right] \right\} + U_{ii} [1 - 2m_{gi}(t)]. \quad (17)$$

Below we assume that the voltage $m_{gj}(t)$ and the control flux $\Phi_j(t)$ (B_j^x field) are varied only on one site with $j = l$, i.e. $m_{gl}(t) = m_l^0 + M_l(t)$. These parameters are constant for all other sites, $m_{gj}(t) = m_j^0$ and $\Phi_j(t) = \Phi^0(2k - 1)/2$, $k = 1, 2, \dots$ for $j \neq l$. Then the Hamiltonian (14) can be written as

$$\mathbf{H}_l(t) = \mathbf{H}^0 + 2M_l(t) \sum_{i=0}^{N-1} U_{li} \mathbf{S}_i^z - B_l^x(t) \mathbf{S}_l^x, \quad (18)$$

where

$$\mathbf{H}^0 = - \sum_{i=0}^{N-1} \mathbf{B}_i^{z,0} \mathbf{S}_i^z. \quad (19)$$

Here

$$\mathbf{B}_i^{z,0} = \sum_{\substack{j=0 \\ j \neq i}}^{N-1} \left[U_{ij} \left(1 - 2m_j^0 - \mathbf{S}_j^z \right) \right] + U_{ii} (1 - 2m_i^0) \quad (20)$$

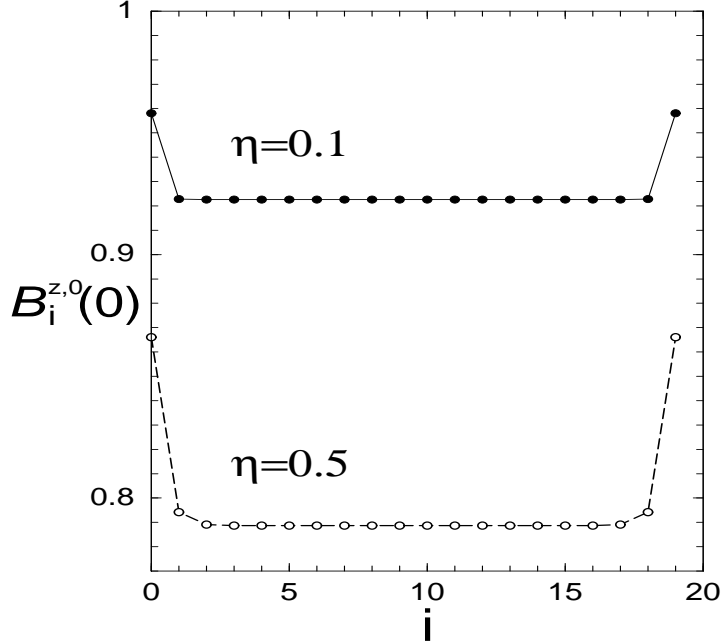


FIG. 2: The static field $B_i^{z,0}(0)$ as a function of the qubit number i for two values of η , $m_j^0 = 0$ ($j = 0, 1, \dots, 19$), $N = 20$.

is the static \mathbf{B}_i^z operator field. The actual static B_i^z field for a state $|p\rangle$ is

$$B_i^{z,0}(p) = \langle p | \mathbf{B}_i^{z,0} | p \rangle = \sum_{\substack{j=0 \\ j \neq i}}^{N-1} \left\{ U_{ij} [1 - 2m_j^0 - s_j^z(p)] \right\} + U_{ii} [1 - 2m_i^0], \quad (21)$$

where the argument p of $B_i^{z,0}(p)$ indicates the state number. This field is nonuniform even for a uniform qubit chain. To illustrate this, we consider the particular example in which all qubits are in the same state $|0\rangle = |00 \dots 00\rangle$ and all static voltages have the same values $m_j^0 = 0$. Then from Eq. (21) one obtains

$$B_i^{z,0}(0) = U_{ii} + \frac{1}{2} \sum_{\substack{j=0 \\ j \neq i}}^{N-1} U_{ij}. \quad (22)$$

In Fig. 2 we plot the static field $B_i^{z,0}(0)$ as a function of the qubit number i for two values of η and for $m_j^0 = 0$, $j = 0, 1, \dots, 19$. The number of qubits is $N = 20$. For a two-qubit chain with the matrix (10) and $a = 1$ one can show that $B_0^{z,0}(0) = B_1^{z,0}(0) \approx 1 - \eta/2$ for $\eta \ll 1$, which is approximately equal to the values of $B_0^{z,0}(0)$ and $B_{N-1}^{z,0}(0)$ in Fig. 2 for $\eta = 0.1$. The static field in Fig. 2 is nonuniform near the edges of the qubit chain despite the fact that all applied voltages have the same values $m_j^0 = 0$ and all qubits are in the same state $|0_j\rangle$.

In dimensional units the total static voltage applied to i th qubit is $v_i^0 = (2e/C_g)(n_i^0 + m_i^0)$. If $n_i^0 = m_i^0 = 0$, then $v^0 = 0$. Due to Eq. (6) the relation between the dimensional magnetic field $B_i^{z,0}(0)$ and the effective static voltage, corresponding to this field, can be written as $(2e^2/C_0)B_i^{z,0}(0) = ev_i^{eff}$. For example, the value $B_i^{z,0}(0) \approx 0.92$ for $i = 1, 2, \dots, N - 2$ and $\eta = 0.1$ in Fig. 2 for $C_0 \approx 500$ aF [4] corresponds to the effective voltage $v_i^{eff} = 0.92 \times 2e/C_0 \approx 0.6$ mV.

IV. THE INTERACTION REPRESENTATION

We decompose the wave function into the basis states $|p\rangle$ of the unperturbed Hamiltonian \mathbf{H}^0 :

$$\psi(t) = \sum_{r=0}^{2^N-1} c_p(t)|p\rangle = \sum_{p=0}^{2^N-1} A_p(t)e^{-iE_p t}|p\rangle, \quad c_p(t) = A_p(t)e^{-iE_p t}, \quad (23)$$

where the Planck constant is $\hbar = 1$, $|p\rangle = |n_{N-1}n_{N-2} \dots n_i \dots n_1 n_0\rangle$, $n_i = 0, 1$, and

$$E_p = \langle p|\mathbf{H}^0|p\rangle = - \sum_{i=0}^{N-1} B_i^{z,0}(p)s_i^z(p). \quad (24)$$

The dimensionless time t in Eq. (23) is expressed in terms of the dimensional time \bar{t} as

$$t = \frac{2e^2}{\hbar C_0} \bar{t}. \quad (25)$$

For $C_0 = 500$ aF, the dimensionless time $t = 1$ corresponds to the dimensional time $\bar{t} \approx 1$ ps, and one dimensionless energy unit corresponds to 0.64 meV.

In the stationary field $B_i^{z,0}(p)$ and when $B_i^x = 0$, the coefficients $A_p(t)$ do not change when time t changes from t' to t'' , *i.e.* $A_p(t'') = A_p(t')$, while the coefficients $c_p(t)$ evolve as $c_p(t'') = c_p(t')e^{-iE_p(t''-t')}$. The representation of the wave function in which the coefficients $A_p(t)$ are used is called the “interaction representation”. Since the coefficients $A_p(t)$ are not changed during the free evolution of the system, the interaction representation allows one to exclude from consideration the dynamics associated with the evolution of the phase of the wave function when no pulses are applied.

V. ONE-QUBIT FLIP

Let us discuss how to implement a resonant one-qubit rotation of the l th qubit for the state $|p\rangle$ in our computer. Initially at the time t_0 the z -component of the magnetic field is $B_l^{z,0}(p)$, and the B_l^x field is switched off, $B_l^x(t_0) = 0$. The flip is implemented in three steps.

(a) One changes the effective voltage $M_l(t)$ (below called voltage) applied to the l th qubit, so that at the end of the pulse of duration $\tau_1 = t_1 - t_0$ the magnitude of $M_l(t)$ becomes $M_l(t_1) = \mathcal{M}_l$. If the transition is resonant \mathcal{M}_l is defined by the resonant condition. [See Eq. (36) below.] From Eq. (18) one can see that after this pulse the B^z field in the location of the l th qubit is

$$B_l^z(p, t_1) = B_l^{z,0}(p) - 2\mathcal{M}_l U_{ll}. \quad (26)$$

Since during the time of application of the first pulse the B_l^x field is turned off, the form of the first pulse is not important, and the relevant parameter is the area $\int_{t_0}^{t_1} M_l(t) dt$ of this pulse which determines phase acquired by the wave function during this pulse. (b) One flips the l th qubit by a rectangular π -pulse with the amplitude B_l^1 and time duration $\tau_2 = t_2 - t_1 = \pi/|B_l^1|$. The B_l^z field is not changed $B_l^z(p, t_2) = B_l^z(p, t_1)$ and $M_l(t_2) = M_l(t_1) = \mathcal{M}_l$. During this pulse the spin flips through the angle π . (c) One restores the voltage applied to the l th qubit from $M_l(t_2) = \mathcal{M}_l$ to its original value $M_l(t_3) = 0$ during the time $\tau_3 = t_3 - t_2$.

First we will discuss the dynamics of the quantum computer during implementation of the steps (a)-(c) in terms of the coefficients $c_p(t)$, then we will formulate the result in the interaction representation in terms of the coefficients $A_p(t)$. Let the l th spin of a state $|p\rangle$ at the initial time t_0 be in the state 0 and the state $|q\rangle$ be related to the state $|p\rangle$ by a flip of the l th spin.

After the first pulse one has

$$c_p(t_1) = e^{-iE_p\tau_1 - i\theta_l^1(p) - i\varphi_l^1} c_p(t_0), \quad c_q(t_1) = e^{-iE_q\tau_1 - i\theta_l^1(p) + i\varphi_l^1} c_q(t_0). \quad (27)$$

The total phase (for the states $|p\rangle$ and $|q\rangle$) $\theta_l^1(p)$ and the phase φ_l^1 are defined by the time-dependent component of the B_l^z field in Eq. (18) as

$$\theta_l^1(p) = 2 \left[\int_{t_0}^{t_1} M_l(t) dt \right] \sum_{\substack{i=0 \\ i \neq l}}^{N-1} U_{li} s_i^z(p), \quad \varphi_l^1 = \left[\int_{t_0}^{t_1} M_l(t) dt \right] U_{ll}. \quad (28)$$

At the end of the first pulse $M_l(t_1) = \mathcal{M}_l$.

After the third pulse, the probability amplitudes become

$$c_p(t_3) = e^{-iE_p\tau_3 - i\theta_l^3(p) - i\varphi_l^3} c_p(t_2), \quad c_q(t_3) = e^{-iE_q\tau_3 - i\theta_l^3(p) + i\varphi_l^3} c_q(t_2). \quad (29)$$

The phases are

$$\theta_l^3(p) = 2 \left[\int_{t_2}^{t_3} M_l(t) dt \right] \sum_{\substack{i=0 \\ i \neq l}}^{N-1} U_{li} s_i^z(p), \quad \varphi_l^3 = \left[\int_{t_2}^{t_3} M_l(t) dt \right] U_{ll}. \quad (30)$$

At the beginning of this pulse, one has $M_l(t_2) = \mathcal{M}_l$, and at the end of the pulse $M_l(t_3) = 0$.

The action of the second rectangular pulse is described by the following Schrödinger equation:

$$\begin{aligned} i\dot{c}_p(t) &= [E_p + b_l(p) + \mathcal{M}_l U_{ll}] c_p(t) - \frac{B_l^1}{2} c_q(t) \\ i\dot{c}_q(t) &= [E_q + b_l(p) - \mathcal{M}_l U_{ll}] c_q(t) - \frac{B_l^1}{2} c_p(t), \end{aligned} \quad (31)$$

where

$$b_l(p) = 2\mathcal{M}_l \sum_{\substack{i=0 \\ i \neq l}}^{N-1} U_{li} s_i^z(p). \quad (32)$$

In order to make the transition $|p\rangle \rightarrow |q\rangle$ resonant, the diagonal elements in Eq. (31) must be equal to each other. The condition

$$E_q - E_p = 2\mathcal{M}_l^r U_{ll} \quad (33)$$

defines the resonant value of the applied voltage \mathcal{M}_l^r . We now calculate the energy difference $E_q - E_p$ using Eq. (24). Since the $B_l^{z,0}(p) = B_l^{z,0}(q)$ and $s_l^z(p) = -s_l^z(q)$, the contribution to the energy difference directly related to the flip of the l th qubit is equal to $B_l^{z,0}(p)$. The states of other qubits with $i \neq l$ are the same for both states, $s_i^z(p) = s_i^z(q)$, but the fields $B_i^{z,0}$, given by Eq. (21), are different due to the influence of the l th qubit measured by the matrix elements U_{li} ,

$$B_i^{z,0}(q) - B_i^{z,0}(p) = - \sum_{\substack{j=0 \\ j \neq i}}^{N-1} U_{ij} [s_j^z(q) - s_j^z(p)] = U_{il}. \quad (34)$$

Finally, we obtain

$$E_q - E_p = B_l^{z,0}(p) - \sum_{\substack{i=0 \\ i \neq l}}^{N-1} U_{li} s_i^z(p). \quad (35)$$

From Eqs. (33) and (35) the resonant value of the applied voltage is

$$\mathcal{M}_l^r = \frac{1}{2U_{ll}} \left[B_l^{z,0}(p) - \sum_{\substack{i=0 \\ i \neq l}}^{N-1} U_{li} s_i^z(p) \right]. \quad (36)$$

Note, that the resonant value of the B_l^z field is not zero because of the constant inter-qubit interaction. From Eqs. (26) and (36) it is equal to

$$B_l^z(p, t_1) = B_l^{z,0}(p) - 2\mathcal{M}_l^r U_{ll} = \frac{1}{2U_{ll}} \sum_{\substack{i=0 \\ i \neq l}}^{N-1} U_{li} s_i^z(p). \quad (37)$$

To find the solution generated by the second pulse, introduce the new coefficients $D_p(\tau)$ and $D_q(\tau)$ as

$$\begin{aligned} c_p(t) &= D_p(\tau)e^{-i[E_p+b_l(p)+\mathcal{M}_l U_{ll}]\tau}, \\ c_q(t) &= D_q(\tau)e^{-i[E_q+b_l(p)-\mathcal{M}_l U_{ll}]\tau}, \end{aligned} \quad (38)$$

where $\tau = t - t_1$. Then, for the coefficients $D_p(\tau)$ and $D_q(\tau)$ one obtains equations

$$\begin{aligned} i\dot{D}_p(\tau) &= -\frac{B_l^1}{2}D_q(\tau)e^{-i\Delta_l\tau}, \\ i\dot{D}_q(\tau_2) &= -\frac{B_l^1}{2}D_p(\tau)e^{i\Delta_l\tau}, \end{aligned} \quad (39)$$

where

$$\Delta_l = E_q - E_p - 2\mathcal{M}_l U_{ll} = B_l^{z,0}(p) - \sum_{\substack{i=0 \\ i \neq l}}^{N-1} U_{li} s_i^z(p) - 2\mathcal{M}_l U_{ll}. \quad (40)$$

The condition $\Delta_l = 0$ is satisfied if the pulse is resonant [see Eq. (36)].

If initially the l th qubit is in the state 0, $D_p(0) = c_p(t_1)$ and $D_q(0) = 0$, the solution of Eq. (39) is

$$\begin{aligned} D_p(\tau_2) &= c_p(t_1) \left[\cos\left(\frac{\lambda_l \tau_2}{2}\right) + i\frac{\Delta_l}{\lambda_l} \sin\left(\frac{\lambda_l \tau_2}{2}\right) \right] e^{-i\frac{\Delta_l}{2}\tau_2}, \\ D_q(\tau_2) &= c_p(t_1) i\frac{B_l^1}{\lambda_l} \sin\left(\frac{\lambda_l \tau_2}{2}\right) e^{i\frac{\Delta_l}{2}\tau_2}, \end{aligned} \quad (41)$$

where $\lambda_l = \sqrt{(B_l^1)^2 + (\Delta_l)^2}$. From Eq. (41) one can see that if $\Delta_l = 0$ and $\tau_2 = \pi/|B_l^1|$ there is a complete transition between the states $|p\rangle$ and $|q\rangle$. Below we call Δ_l for state $|p\rangle$ the detuning for this state.

We now express these results in the interaction representation in terms of the coefficients $A_p(t)$. Let the state $|p\rangle$ with l th qubit in the state $|0_l\rangle$ be populated at time $t = t_0$. From the second expression in Eq. (23) and the first expression in Eq. (27) one obtains

$$c_p(t_0) = A_p(t_0)e^{-iE_p t_0}, \quad c_p(t_1) = A_p(t_0)e^{-iE_p t_1 - i\theta_l^1(p) - i\varphi_l^1}. \quad (42)$$

Taking into consideration Eqs. (38), (40), and (41), one has

$$\begin{aligned} c_p(t_2) &= A_p(t_0) \left[\cos\left(\frac{\lambda_l \tau_2}{2}\right) + i\frac{\Delta_l}{\lambda_l} \sin\left(\frac{\lambda_l \tau_2}{2}\right) \right] e^{i\left\{-E_p t_2 - \theta_l^1(p) - \varphi_l^1 - \left[b_l(p) + \mathcal{M}_l U_{ll} + \frac{\Delta_l}{2}\right]\tau_2\right\}}, \\ c_q(t_2) &= A_p(t_0) i\frac{B_l^1}{\lambda_l} \sin\left(\frac{\lambda_l \tau_2}{2}\right) e^{i\left\{-E_q t_2 - \theta_l^1(p) - \varphi_l^1 - \left[b_l(p) + \mathcal{M}_l U_{ll} + \frac{\Delta_l}{2}\right]\tau_2 + (\Delta_l + 2\mathcal{M}_l U_{ll})t_2\right\}}. \end{aligned} \quad (43)$$

Finally, using Eq. (29) one obtains in the interaction representation

$$\begin{aligned}
 A_p(t_3) &= A_p(t_0) \left[\cos\left(\frac{\lambda_l \tau_2}{2}\right) + i \frac{\Delta_l}{\lambda_l} \sin\left(\frac{\lambda_l \tau_2}{2}\right) \right] e^{i[\Theta_l(p) - \theta_l^3(p) - \varphi_l^3]}, \\
 A_q(t_3) &= A_p(t_0) i \frac{B_l^1}{\lambda_l} \sin\left(\frac{\lambda_l \tau_2}{2}\right) e^{i[\Theta_l(p) - \theta_l^3(p) + \varphi_l^3 + (\Delta_l + 2\mathcal{M}_l U_l) t_2]},
 \end{aligned} \tag{44}$$

where the common phase

$$\Theta_l(p) = -\theta_l^1(p) - \varphi_l^1(p) - \left[b_l(p) + \mathcal{M}_l U_l + \frac{\Delta_l}{2} \right] \tau_2 \tag{45}$$

depends on the parameters of the first two pulses and on the initial state $|p\rangle$.

A. Calculation of the detuning Δ_l

Assume that initially there are two states, $|r\rangle$ and $|R\rangle$, in the quantum register and assume $\Delta_l = 0$ for the state $|R\rangle$ and $\Delta_l \neq 0$ for the state $|r\rangle$: the B^x pulse is resonant for the state $|R\rangle$ and nonresonant for the state $|r\rangle$. The value of Δ_l for the state $|r\rangle$ can be found from Eqs. (36) and (40),

$$\Delta_l(r, R) = -2 \sum_{\substack{i=0 \\ i \neq l}}^{N-1} U_{li} [s_i^z(r) - s_i^z(R)]. \tag{46}$$

This equation can serve as a general definition of the detuning Δ_l for an arbitrary state $|r\rangle$ expressed through the eigenvalues of \mathbf{S}_i^z for this state and the eigenvalues of this operators for the state $|R\rangle$, for which the transition is resonant. From Eq. (46) one can see that in general $\Delta_l(r, R)$ is independent of the static voltages m_j^0 , and for a resonant transition $\Delta_l(R, R) = 0$.

VI. PROTOCOL FOR CREATION OF ENTANGLED STATE

Let the initial state be the state $|0_{N-1}0_{N-2}\dots 0_10_0\rangle$. If $\eta \ll 1$ this is the ground state when the applied B^z field is oriented in the positive z -direction, *i.e.* when $0 \leq m_i^0 < 1/2$. (See Fig. 2 for the case $m_i^0 = 0$.) Using the Hadamard transform G_H we split the ground state into two states

$$G_H|0_{N-1}0_{N-2}\dots 0_10_0\rangle = \frac{1}{\sqrt{2}}(|0_{N-1}0_{N-2}\dots 0_10_0\rangle + |0_{N-1}0_{N-2}\dots 0_11_0\rangle). \tag{47}$$

Here and below we omit the total phase factor. During the next step, we flip the first qubit in the excited state and do not flip the same qubit in the ground state to obtain the state

$$\frac{1}{\sqrt{2}}(|0_{N-1}0_{N-2}\dots 0_10_0\rangle + |0_{N-1}0_{N-2}\dots 0_21_11_0\rangle). \quad (48)$$

Repeating the latter procedure for the remaining $N - 2$ qubits we will obtain the entangled state:

$$\frac{1}{\sqrt{2}}(|0_{N-1}0_{N-2}\dots 0_10_0\rangle + |1_{N-1}1_{N-2}\dots 1_11_0\rangle). \quad (49)$$

We now define the parameters of the pulses required to implement this protocol.

A. Hadamard gate

Assume that initially, at time t_0 , there is only the ground state $|0\rangle = |00\dots 00\rangle$ in the register. The Hadamard transform is implemented using the sequence of the pulses (a)-(c) described in Sec.V. In step (b) instead of π pulse we apply a $\pi/2$ -pulse.

The form and duration of the first pulse are not important, since they affect only the total phase of the wave function. What is important is the value of the $B_0^z(0, t_1)$ field after this pulse. To make this field equal to the resonant value (resonant pulse) one should apply the voltage

$$\mathcal{M}_0^r = \frac{1}{2U_{00}} \left[B_0^{z,0}(0) - \sum_{i=1}^{N-1} U_{0i} s_i^z(0) \right], \quad (50)$$

where $s_i^z(0) = 1/2$, and we used Eq. (36). During the second pulse one keeps the gate voltage constant. For the case $m_j^0 = 0$ one has $\mathcal{M}_0^r = 1/2$. The second rectangular $\pi/2$ -pulse with the amplitude B_l^1 has the duration $\tau_2 = \pi/(2|B_l^1|)$. A specific value of B_l^1 is not important. The only condition is $B_l^1 \neq 0$.

During the third pulse the voltage is changed from \mathcal{M}_0^r in Eq. (50) to its original value which is equal to zero. To equalize the phases of two states of the superposition, the condition

$$-\varphi_0^3 = \varphi_0^3 + [\Delta_0(0, 0) + 2\mathcal{M}_0^r U_{00}]t_2 + \frac{\pi}{2} \quad (51)$$

must be satisfied [see Eq. (44)]. Here $\Delta_0(0, 0) = 0$. If we set initially $t_0 = 0$, then

$$t_2 = \tau_1 + \tau_2 = \tau_1 + \frac{\pi}{2|B_0^1|}. \quad (52)$$

This gives us the last parameter of the Hadamard gate

$$\varphi_0^3 = -\mathcal{M}_0^r U_{00} \left(\tau_1 + \frac{\pi}{2|B_0^1|} \right) - \frac{\pi}{4}. \quad (53)$$

B. Conditional flip

All other steps of the protocol implement flips of the 1st, 2nd \dots , $(N - 2)$ th, $(N - 1)$ th qubits in the excited state and suppress flips of these qubits in the ground state. We will derive the parameters required to implement this operation for the first qubit. The parameters required to flip the other $N - 2$ qubits can be obtained in a similar way. Note that the parameters required to flip different qubits are different even for a homogeneous spin chain because the static B^z field $B_i^{z,0}(R)$ is different for different qubits i and states $|R\rangle$, and because the phase factor $\exp[i2\mathcal{M}_l U_{ll} t_2]$ in Eq. (44) depends on the history of the excited state.

Before the pulses (a)-(c) are applied, there are two states in the register $|r\rangle = |00\dots 00\rangle$ and $|R\rangle = |00\dots 01\rangle$. As for the Hadamard transform, the form and duration of the first pulse is unimportant. The value of the voltage after this pulse is

$$\mathcal{M}_1^r = \frac{1}{2U_{11}} \left[B_1^{z,0}(R) - \sum_{\substack{i=0 \\ i \neq 1}}^{N-1} U_{1i} s_i^z(R) \right]. \quad (54)$$

If $m_j^0 = 0$, then

$$\mathcal{M}_1^r = \frac{1}{2} + \frac{U_{10}}{U_{11}}. \quad (55)$$

The second rectangular π -pulse with the amplitude B_1^1 has the duration $\tau_2 = \pi/(|B_1^1|)$. In order to suppress the nonresonant transition $|00\dots 000\rangle \rightarrow |00\dots 010\rangle$ from the ground state, the value of $|B_1^1|$ must satisfy the $2\pi K$ -condition [20]

$$B_1^1 = \pm \frac{\Delta_1(r, R)}{\sqrt{4K^2 - 1}}, \quad K = 1, 2, \dots, \quad (56)$$

where B_1^1 can be positive or negative. For this particular pulse, using Eq. (46), one obtains $\Delta_1(r, R) = -2U_{10}$. If B_1^1 satisfies Eq. (56) the value of the sine in Eq. (44) becomes zero, and the nonresonant transition is suppressed.

The voltage $M_1(t)$ is switched off, $\mathcal{M}_1^r \rightarrow 0$, and the phase is corrected by the third pulse, for which the condition

$$\Theta_1(r) - \varphi_1^3 \left[1 + \frac{2}{U_{11}} \sum_{\substack{i=0 \\ i \neq 1}}^{N-1} U_{1i} s_i^z(r) \right] + K\pi = \varphi_1^3 \left[1 - \frac{2}{U_{11}} \sum_{\substack{i=0 \\ i \neq 1}}^{N-1} U_{1i} s_i^z(R) \right] + \Theta_1(R) + 2\mathcal{M}_1 U_{11} t_2 + \frac{\pi}{2} \quad (57)$$

must be satisfied. Here $t_2 = T_1 + \tau_1 + \tau_2$, and T_1 is the time of the beginning of the current three-pulse sequence. Finally, the phase is

$$\varphi_1^3 = \frac{\Theta_1(r) - \Theta_1(R) - 2\mathcal{M}_1 U_{11} t_2 + (K-1)\frac{\pi}{2}}{2 - \frac{2}{U_{11}} \sum_{\substack{i=0 \\ i \neq 1}}^{N-1} U_{1i} [s_i^z(R) - s_i^z(r)]} = \frac{\Theta_1(r) - \Theta_1(R) - 2\mathcal{M}_1 U_{11} t_2 + (K-1)\frac{\pi}{2}}{2 + \frac{2U_{10}}{U_{11}}}. \quad (58)$$

VII. COMMENTS ON PRACTICAL IMPLEMENTATION

The protocol discussed in this paper provides the parameters for exact implementation of entanglement in a chain of many coupled SQUIDs. We demonstrated that the phase of the wave function can be controlled by controlling the gate voltages. In a practical situation one of the objectives can be the creation of the entangled state with a relatively large constant of interaction between qubits (but not using this state for implementation of more complicated quantum algorithms). If the creation of the entangled state is the purpose of an experiment, then the phases of the entangled states can not be important. In this situation, there is no need to control the phase φ_l^3 , and the important parameters are: (i) the value of the gate voltage \mathcal{M}_l applied to the qubit to be flipped, (ii) the amplitude B_l^1 and (iii) the time-duration τ_2 of B^x pulse [controlled by the magnetic flux $\Phi_l(t)$].

We now make some remarks concerning the specific field configuration that we chose in this paper for implementation of quantum logic. First, all qubits are initially placed in a permanent static B^z field, $B_j^{z,0} \neq 0$ created by static voltages m_j^0 and the inter-qubit interaction. Before a flip of the l th qubit by a B^x pulse, the voltage applied to this qubit is switched to the resonant value, and after the B^x -pulse this voltage is switched to its initial value. As follows from the results of this paper, the nonzero static $B_j^{z,0}$ field introduces an additional parameter, or degree of freedom: by changing this field it is possible to control the phase of the wave function.

The qubit rotations are implemented by the rectangular B_l^x -pulses because during implementation of these pulses the effective B_l^z field in the location of the l th qubit is not equal to zero for some quantum states of the superposition. That is why the result of the action of a B^x -pulse on the states with nonzero B_l^z field depends on the form of this pulse. The analytic solution is known for a rectangular pulse, so the rectangular form of the B_l^x -pulse is the simplest possible choice that allows one to analyze the basic properties of the system

and optimize the parameters of the pulses.

The interaction representation used in this paper for modeling of quantum logic is employed because it effectively eliminates from consideration free quantum dynamics of the quantum states of the superposition. Namely, since different states of the superposition have different energies E_p , they acquire different phase factors even in the case when the applied fields are not changed. The interaction representation allows one to choose the static voltages m_i^0 arbitrarily. In particular, one can choose $m_i^0 = 0$. (See, for example, Fig. 2 of this paper.) If $n_i^0 = 0$, this would allow one to decrease the decoherence effect of the gate because the gate voltage is switched on and off only during the logic operation on a specific qubit. Also the time between the pulses can be chosen arbitrarily because the wave amplitudes in the interaction representation are not changed during this time.

VIII. LONG-RANGE INTERACTION

For two states in the register, the system with long-range interaction between qubits is exactly solvable. However, the universal quantum computation involving an arbitrary possible number of states in the quantum register is supposed to be implemented by taking into consideration only nearest neighbor interaction. The long-range interaction in the general case results in generation of error states. These errors are small only when the value of η , characterizing the coupling strength, is small. For example, the value $\eta = 0.1$ can be considered as large because the long-range interaction produces the error of the order $\eta = 0.1$ in the probability amplitude and phase of the wave function. In order to show this, consider Eq. (44). Due to Eq. (46) the contribution of $(l - 2)$ th and $(l + 2)$ th qubits to the detuning Δ is of order η^2 ; the contribution of $(l - 3)$ th and $(l + 3)$ th qubits to the detuning Δ is of order η^3 , and so on. If the parameters of the pulses are calculated by taking into consideration only nearest neighbors, instead of the resonant transition with $\Delta = 0$ one has an almost resonant transition (for $\eta \ll 1$) with the nonzero detuning $\Delta \sim \eta^2$ created by $(l - 2)$ th and $(l + 2)$ th qubits. Since in Eq. (44) $\lambda_l \sim \eta$, the relation Δ_l/λ_l is of order of η ; the value of the sine (for almost resonant transition) is of order of unity; so that the error in the probability amplitude and phase of the wave function is of order η .

In order to calculate the error introduced by the long-range interaction, we numerically simulated the creation of entanglement. The parameters of the pulses were calculated by

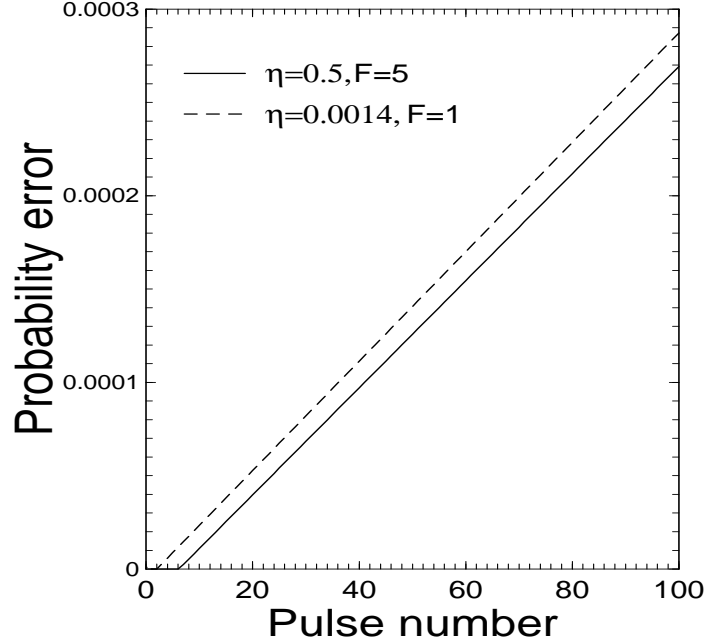


FIG. 3: The probability error as a function of B^x pulse number. $N = 100$, $K = 1$; $m_j^0 = 0$, $j = 0, 1, \dots, N - 1$.

taking into consideration only F nearest neighbors, $F = 1, 2, \dots$. We define the probability error as

$$\mathcal{P}(t) = \left| |A_r(t)|^2 - \frac{1}{2} \right| + \left| |A_R(t)|^2 - \frac{1}{2} \right|, \quad (59)$$

and plot it as a function of the number of B^x pulses in Fig. 3. The total number of B^x pulses is equal to the number of qubits N in the chain. In Eq. (59) $|r\rangle$ is the ground state and $|R\rangle$ is the excited state.

The probability error $\mathcal{P}(t)$ in Fig. 3 generated by one pulse is equal, on average, to 2.87×10^{-6} (9.77×10^{-4}) for $F = 5$ and $\eta = 0.5$; and $\mathcal{P} = 2.93 \times 10^{-6}$ (1.96×10^{-6}) for $F = 1$ and $\eta = 0.0014$. In brackets we indicate the values calculated using the analytical estimates presented in the beginning of this section. Namely, the error in the probability amplitude is of the order η^F , and the error in the probability is of order η^{2F} . The poor correspondence between estimated and numerical results for $\eta = 0.5$ follows from the fact that for relatively large η the off-diagonal matrix elements in the matrix U_{ij} decrease faster than $\eta^{|i-j|}$, $i \neq j$.

As follows from Fig. 3, in order to decrease the error one can (i) take into consideration a larger number of nearest neighbors or (ii) decrease the coupling constant η . The results

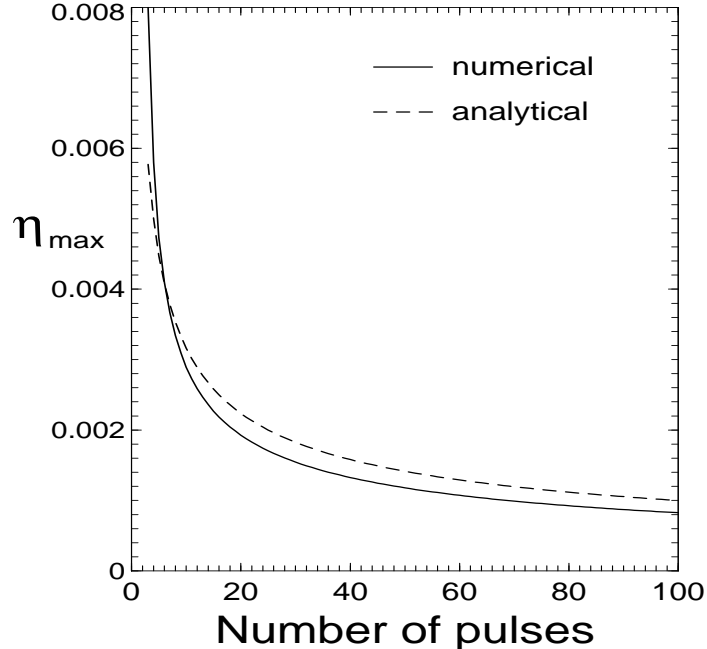


FIG. 4: The maximum value of η (y -axis) required to implement the entanglement protocol using N pulses (x -axis), with the probability error less than $\mathcal{P}_0 = 10^{-4}$. $F = 1$, $K = 1$; $m_j^0 = 0$, $j = 0, 1, \dots, N - 1$. The solid curve is obtained using Eq. (44) and the dashed curve is obtained using Eq.(61).

presented in Fig. 3 can be used to estimate the probability error in more complex protocols with the same values of F and η , since one can assume that this error mostly depends on the number of B^x pulses and not on a particular protocol.

As shown in this paper, the effects of the long-range interaction can be completely compensated by choosing the optimal values of the B^z and B^x fields when the number of useful states in the quantum register is equal to 2. In the general case of an arbitrary (possible) number of states in the register, only the nearest neighbors can be taken into consideration, and the long-range interaction can be suppressed only by decreasing the value of η . In Fig. 4 we plot the maximum value η_{\max} required to implement the protocol for creation of entanglement using N pulses with the probability error less than $\mathcal{P}_0 = 10^{-4}$ when only the nearest neighbors are taken into consideration, $F = 1$.

The value of η_{\max} in Fig. 4 can be estimated analytically. As follows from Fig. 3 the error accumulates linearly with the number of pulses, so that we can write

$$\mathcal{P}_0 = N\mathcal{P}' = N\eta_{\max}^2, \quad (60)$$

where \mathcal{P}' is the error generated by one pulse. From Eq. (60) the maximum value of η required to implement an N -pulse protocol with the accuracy $\mathcal{P}_0 = 10^{-4}$ is

$$\eta_{\max} = \sqrt{\frac{\mathcal{P}_0}{N}} = \frac{0.01}{\sqrt{N}}. \quad (61)$$

From Fig. 4 one can see that our analytical estimate for η_{\max} is close to the exact result obtained using numerical simulations.

Decreasing η decreases the error. On the other hand, since η defines the clock speed of the quantum computer (the time of implementation of one B^x pulse is of order of π/η), decreasing η slows the computer down. This can lead to an accumulation of errors introduced by the environment. The optimal value of η can be estimated by taking into consideration both the effect of the long-range interaction and the influence of the environment.

IX. CONCLUSION

We considered in this paper an optimal implementation of quantum logic operations for a scalable superconducting quantum computer with constant inter-qubit interaction. The protocol for creation of entanglement with arbitrary number of qubits was analyzed in detail, for a relatively large interaction constant. A possible application of our approach for implementing universal quantum logic for more complex algorithms by decreasing the coupling constant and, correspondingly, decreasing the clock speed was discussed. The errors introduced by the long-range interaction for the universal logic gates are estimated analytically and calculated numerically. The coherent charge oscillations in this model have already been observed experimentally [4]. A further feasible accomplishment would be the experimental creation of entanglement in a system with three qubits. A demonstration of the entanglement in the potentially scalable QC architecture with the superconducting qubits would be an important step toward the experimental implementation of a scalable QC with many qubits.

Acknowledgments

We thank G.D. Doolen for discussions. This work was supported by the Department of Energy under the contract W-7405-ENG-36 and DOE Office of Basic Energy Sciences,

by the National Security Agency (NSA) and Advanced Research and Development Activity (ARDA) under Army Research Office (ARO) contract # 707003.

APPENDIX A: CREATION OF ENTANGLEMENT WITH TWO QUBITS

Let us calculate the parameters required to create the entanglement in the chain of two qubits starting from the state $|00\rangle$ and using the parameters from the experimental system [4]. We will not calculate the phase φ_l^3 required to implement the phase correction, since it depends on particular forms of the gate pulses $M_l(t)$, and calculate the parameters required to create the entanglement without phase correction. There are three devices attached to i th ($i = 0, 1$) SQUID: superconducting electrode with the capacitance C_{Ji} , electrostatic gate with the capacitance C_{gi} , and a probe with the capacitance C_{bi} . We assume that during implementation of the protocol the probe voltages V_{bi} are switched off, so that the charges $Q_{bi} = C_{bi}V_{bi}$ induced by the probes are equal to zero. The capacitances are

$$C_{J0} = 620 \text{ aF}, \quad C_{g0} = 0.60 \text{ aF}, \quad C_{b0} = 41 \text{ aF}, \quad C_0 = C_{J0} + C_{g0} + C_{b0} = 661.6 \text{ aF}. \quad (\text{A1})$$

$$C_{J1} = 460 \text{ aF}, \quad C_{g1} = 0.61 \text{ aF}, \quad C_{b1} = 50 \text{ aF}, \quad C_1 = 510.61 \text{ aF}. \quad (\text{A2})$$

The coupling capacitance C_c and the coupling constant η are

$$C_c = 34 \text{ aF}, \quad \eta = \frac{C_c}{C_0} = \frac{34}{661.6} \approx 5.139 \times 10^{-2}. \quad (\text{A3})$$

The coupling matrix U_{ij} , $i, j = 0, 1$, is given by Eq. (10), where

$$a = \frac{C_1}{C_0} = \frac{510.61}{661.6} \approx 0.7718. \quad (\text{A4})$$

The dimensionless parameters η and a and the dimensionless static voltages m_0^0 and m_0^1 completely define the parameters of the protocol.

The value of the voltage \mathcal{M}_0 applied to the zeroth qubit is given by Eq. (36),

$$\mathcal{M}_0^r = \frac{1}{2} - m_0^0 - \frac{U_{01}}{U_{00}} m_1^0. \quad (\text{A5})$$

The amplitude B_0^1 of the applied B^x field is arbitrary, and the time-duration of this pulse is

$$\tau_2 = \frac{\pi + 2\pi k}{2|B_0^1|}, \quad k = 0, 1, 2, \dots \quad (\text{A6})$$

The gate voltage \mathcal{M}_1 for the second pulse is

$$\mathcal{M}_1^r = \frac{1}{2} - m_1^0 + \frac{U_{10}}{U_{11}}(1 - m_0^0). \quad (\text{A7})$$

The magnitude of Δ_1 calculated using Eq. (46) is $-2U_{01}$, and the amplitude of B^x field is

$$B_1^1 = \frac{2U_{01}}{\sqrt{4K^2 - 1}}, \quad K = 1, 2, \dots \quad (\text{A8})$$

The time-duration of the second B^x pulse is

$$\tau_2 = \frac{\pi + 2\pi k}{|B_1^1|}, \quad k = 0, 1, 2, \dots \quad (\text{A9})$$

APPENDIX B: CREATION OF ENTANGLEMENT WITH THREE QUBITS

The matrix U_{ij} for the system of three identical qubits is given by Eq. (12). The protocol presented in this Appendix is also valid for a system with nonidentical qubits. The gate voltage \mathcal{M}_0 for the first B^x pulse is

$$\mathcal{M}_0^r = \frac{1}{2} - m_0^0 - \frac{U_{01}}{U_{00}}m_1^0 - \frac{U_{02}}{U_{00}}m_2^0. \quad (\text{B1})$$

The magnitude of B_0^1 is arbitrary, and τ_2 is given by Eq. (A6).

The gate voltage \mathcal{M}_1 for the second pulse is

$$\mathcal{M}_1^r = \frac{1}{2} - m_1^0 + \frac{U_{10}}{U_{11}}(1 - m_0^0) - \frac{U_{12}}{U_{11}}m_2^0. \quad (\text{B2})$$

The magnitudes of $\Delta_1 = -2U_{01}$, B_1^1 , and τ_2 for the second pulse are given by the same formulas (A8) and (A9) as for the case of two qubits.

The gate voltage \mathcal{M}_2 for the third pulse is

$$\mathcal{M}_2^r = \frac{1}{2} - m_2^0 + \frac{U_{20}}{U_{22}}(1 - m_0^0) + \frac{U_{21}}{U_{22}}(1 - m_1^0). \quad (\text{B3})$$

The detuning Δ_2 for the third pulse is $-2U_{20} - 2U_{21}$, and the amplitude of B^x field is

$$B_2^1 = \frac{2U_{20} + 2U_{21}}{\sqrt{4K^2 - 1}}, \quad K = 1, 2, \dots, \quad (\text{B4})$$

The time-duration of the third B^x pulse is

$$\tau_2 = \frac{\pi + 2\pi k}{|B_2^1|}, \quad k = 0, 1, 2, \dots \quad (\text{B5})$$

[1] Y. Makhlin, G. Schön, and A. Shnirman, Rev. Mod. Phys. **73**, 357 (2001).

- [2] I. Chiorescu, Y. Nakamura, C.J.P.M. Harmans, and J. E. Mooij, *Science* **299**, 1869 (2003).
- [3] Y. Nakamura, Yu. A. Pashkin, and J. S. Tsai, *Nature* **398**, 786 (1999).
- [4] Yu. A. Pashkin, T. Yamamoto, O. Astafiev, Y. Nakamura, D. V. Averin, and J. S. Tsai, *Nature* **421**, 823 (2003).
- [5] R. C. Ramos, F. W. Strauch, P. R. Johnson, A. J. Berkley, H. Xu, M. A. Gubrud, J. R. Anderson, C. J. Lobb, A. J. Dragt, and F. C. Wellstood, *IEEE Trans. on Appl. Supercond.* **13**, 994 (2003).
- [6] J. M. Martinis, S. Nam, J. Aumentado, and C. Urbina, *Phys. Rev. Lett.* **89**, 117901 (2002).
- [7] Y. Yu, S. Han, X. Chu, S. Chu. and Z. Wang, *Science* **296**, 889 (2002).
- [8] Y. Makhlin, G. Schön, and A. Shnirman, *Nature* **386**, 305 (1999).
- [9] F. Plastina, R. Fazio, and G. M. Palma, *Phys. Rev. B* **64**, 113306 (2001).
- [10] J. Q. You, C.-H. Lam, and H. Z. Zheng, *Phys. Rev. B* **63**, 180501 (2001).
- [11] J. Q. You, J. S. Tsai, and F. Nori, *Phys. Rev. Lett.* **89**, 197902 (2002).
- [12] A. Blais, A. M. van den Brink, and A. M. Zagoskin, *Phys. Rev. Lett.* **90**, 127901 (2003).
- [13] P. R. Johnson, F. W. Strauch, A. J. Dragt, R. C. Ramos, C. J. Lobb, J. R. Anderson, and F. C. Wellstood, *Phys. Rev. B* **67**, 020509 (2003).
- [14] F. Plastina and G. Falci, *Phys. Rev. B* **67**, 224514 (2003).
- [15] Y. Nakamura, Yu. A. Pashkin, and J. S. Tsai, *Phys. Rev. Lett.* **87**, 246601 (2001).
- [16] Y. Nakamura, Yu. A. Pashkin, and J. S. Tsai in: *Macroscopic Quantum Coherence and Quantum Computing*, Eds. D. V. Averin, B. Ruggiero, and P. Silvestrini, p. 17 (Kluwer Academic/Plenum Publishers, New York, 2001)
- [17] C. Granata, V. Corato, A. Monaco, B. Ruggiero, M. Russo, and P. Silvestrini, *Appl. Phys. Lett.* **79**, 1145 (2001).
- [18] C. Bruder, R. Fazio, and G. Schön, *Phys. Rev. B* **47**, 342 (1993).
- [19] L. I. Glazman and A. I. Larkin, *Phys. Rev. Lett.* **79**, 3736 (1997).
- [20] G. P. Berman, D. K. Campbell, and V. I. Tsifrinovich, *Phys. Rev. B* **55**, 5929 (1997).